

# Magnification factor for adaptation of a visual transient mechanism

Stuart Anstis

*Department of Psychology, York University, 4700 Keele Street, North York M3J 1P3, Canada*

John Harris

*Brain and Perception Laboratory, Medical School, University Walk, University of Bristol, Bristol BS8 1TD, England*

Received January 27, 1987; accepted April 1, 1987

After adaptation by an observer to a patch of gradually increasing (or decreasing) luminance, a steady test patch appeared to be gradually dimming (or brightening). These aftereffects did not transfer interocularly. Adaptation to a checkerboard, in which the white squares gradually dimmed while the black squares gradually brightened, gave an aftereffect that was a pattern of intersecting diagonal lines, that is, an extremely blurred checkerboard. The larger the squares of the checkerboard were, the farther into the periphery the aftereffect extended, because small squares were blurred out by the summation areas of the underlying visual channels, which were larger at increasing eccentricities and had diameters of 20 times the resolvable dot separation. The estimated visual acuity of these channels was as low as 20/400. These estimates were confirmed by manipulating separately the local and space-averaged luminances of the adapting stimulus.

## INTRODUCTION

An earlier paper<sup>1</sup> described a visual aftereffect produced by adaptation to gradual change in luminance.<sup>2,3</sup> After adaptation to a uniform field that was growing gradually brighter, a subsequently viewed steady test field appeared to be growing gradually dimmer. Conversely, after adaptation to a dimming field, a steady test field appeared to grow gradually brighter (Fig. 1). Presumably the aftereffects selectively adapt on and off transient visual channels that respond to gradual changes in luminance. The adaptation is to a change in luminance, not to a change in hue; exposure to a light whose wavelength swept gradually through the spectrum produced no aftereffects of apparent color change.<sup>4</sup> An adapting field of constant luminance, which appears to be brightening owing to lateral brightness induction from an adjacent dimming field, can produce a dimming aftereffect.<sup>4,5</sup> Hence the site of the aftereffect must lie after the lateral inhibitory processes that govern brightness induction. There is evidence that the output of these transient channels is integrated and fed back into the perception of steady luminance levels<sup>6</sup> and also that their outputs are fed forward to provide inputs into the visual channels that respond to motion.<sup>7</sup>

In this paper we present six experiments. The first three examine the spatial properties of this aftereffect as a function of retinal eccentricity, and the other three are informal demonstrations of its monocular, rather than binocular, basis.

## EXPERIMENTS

### Experiment 1: Spatial Properties of the Aftereffects

The stimuli were displayed on a color television (TV) monitor controlled by a microcomputer.<sup>8</sup> The diagonal of the TV

screen subtended 28 deg of visual angle at a viewing distance of 57 cm in a dimly lit room. Checkerboard patterns were displayed on the TV screen, and different squares were independently modulated with rising or falling luminance ramps such that the white squares gradually darkened while the black squares gradually lightened. In practice, each ramp was approximated by a staircase of 16 luminance steps. Brightening ramps increased gradually in luminance one step at a time from black ( $0.2 \text{ cd m}^{-2}$ ) to white ( $118 \text{ cd m}^{-2}$ ) and then fell back to black and recycled. Dimming ramps did the opposite. The computer put out 16 equally spaced voltage steps, but the luminance output from the monitor phosphor was proportional to the 2.33rd power of the input. The side of each square subtended 2.5-deg visual angle, and the ramp repetition rate was 2.3 Hz. Subjects fixated a small red dot in the middle of the screen while they adapted for 30 sec to the checkerboard display of brightening and dimming squares. The display then switched to a steady uniform mid-gray test field ( $28 \text{ cd m}^{-2}$ ). Subjects reported a strong aftereffect, in which the previously dimming squares appeared (1) to be growing brighter and (2) to be of higher mean brightness<sup>6</sup> compared with the previously brightening squares, which appeared (1) to be growing dimmer and (2) to be of lower mean brightness.<sup>6</sup> The aftereffect grew stronger during the test period, reaching a peak 1–2 sec after the end of adaptation and vanishing shortly thereafter. These aftereffects were not repetitive, like the sawtooth adapting stimuli; they consisted of a single slow apparent ramp of brightness increase or decrease. The effects were very robust and often drew exclamations of surprise from first-time viewers.

The aftereffect regions were blurred light and dark apparent blobs, centered on the positions of the adapting squares and connected by diagonal bands, as in a diagonal plaid or gingham pattern (Fig. 2). In other words, the test patch

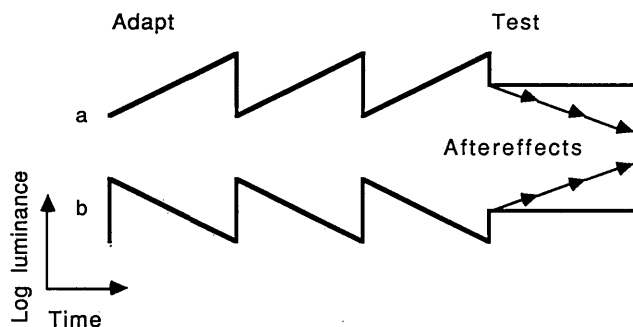


Fig. 1. a, After adaptation by the observer to a spatially uniform brightening field whose luminance is modulated with a rising ramp, a steady test field (horizontal line at right) appears to be drifting downward in luminance (dashed arrow). b, Similarly, adaptation to a dimming field gives rise to an aftereffect of apparent brightening (lower dashed arrow).<sup>1</sup>

resembled a checkerboard from which the high spatial frequencies have been filtered out. A checkerboard contains no Fourier components parallel to the edges of its squares. Its Fourier fundamentals lie along the 45-deg diagonals, and removing the upper harmonics makes the diagonal fundamental spatial-frequency components stand out.

Thus an adapting checkerboard whose squares were luminance modulated by ramps in counterphase produced aftereffect regions that were strongly blurred. This blurring was far more severe than in a conventional afterimage. This was verified by inducing a conventional afterimage and our dimming or brightening aftereffect simultaneously from the same adapting pattern. The brightening squares were made green (Commission International de L'Eclairage coordinates  $x = 0.327$ ,  $y = 0.578$ ), and the dimming squares were made magenta ( $x = 0.268$ ,  $y = 0.130$ ), or vice versa. After adaptation by the observer, the afterimage seen consisted of a sharp-edged checkerboard in complementary colors. Superimposed upon this afterimage was a blurred spatial pattern of brightening and dimming aftereffects. Since the aftereffects were significantly more blurred than the afterimage, we conclude that the blurring in the aftereffects was not caused by the slow diffusive blurring of photopigment that can gradually affect afterimages,<sup>9</sup> by optical factors, or by eye movements; it is likely that the blurring indicates the spatial properties of the specific neural mechanisms that were being adapted. These are the topic of our study.

As one would expect, the blur process affected small checkerboard squares more severely than large squares. We reduced the sides of the squares fourfold, from 2.5 to 0.62 deg, and found that the aftereffect was now fainter and more fugitive, reaching its peak immediately, instead of after a 1–2-sec delay, and dying away rapidly. The aftereffect had a quality of rapidly scurrying random apparent motion, unlike the slow blooming produced by the larger adapting squares.

A second consequence of reducing the size of the squares was to confine the aftereffects to a smaller retinal region around the fovea (Figs. 2b–2d). (On the other hand, pilot work showed that the afterimage from a checkerboard of 0.62-deg squares was not restricted to a parafoveal region but covered the same retinal region as the 28-deg adapting stimulus.)

We attribute this restriction in the area of the aftereffect to the increasing coarseness of the retinal grain (Fig. 2e) with

greater eccentricity.<sup>10–17</sup> At eccentricities where the perceptive fields<sup>14,15</sup> of the adapting mechanisms are larger than the squares, the opposite aftereffects in adjacent squares will blur together, and no aftereffect pattern will be seen. We predict that the aftereffect will cancel when the summation area receives equal areas of brightening and dimming squares so that it receives equal and opposite changes in luminance over time, which will cancel out. This condition is met by a summation area as large as two stimulus squares, for instance, a hypothetical diamond-shaped receptive field (RF) whose side is  $\sqrt{2}$  times that of the threshold checkerboard square (Fig. 2c). (Real perceptive fields are likely to be circular.) Since RF's systematically increase in size with eccentricity, we predict that larger checkerboard squares will give aftereffects that extend farther out into the retinal periphery. We verified this prediction by adapting our subjects to checkerboard squares of various sizes.

We used seven subjects, of whom six were naive about the purpose of the experiment. A readaptation procedure was used, in which the subject initially adapted to the checkerboard for 30 sec and then viewed a static gray test field for 2 sec alternating with the adapting checkerboard for 8 sec, and so on. The adapting checkerboard always filled the entire monitor screen and was 22.5 deg wide and 17 deg high, but the aftereffect usually appeared to fill only a disk-shaped region, centered on the fovea, that was smaller than the checkerboard. The subject set an electronic pointer on the TV screen to mark the perceived right-hand edge of the aftereffect region during the test periods. Although unlimited time was allowed, a typical setting required 30–40 sec. Six sizes of checkerboard square, 0.2, 0.3, 0.5, 0.7, 1.0, and 1.3 deg, were presented twice each in random order. Subjects rested for at least 5 min between each setting to reduce carryover effects.

Results are shown in Fig. 3. Each point is the mean of 14 readings (seven subjects, two trials each). Figure 3 shows that larger squares gave a larger retinal region of aftereffect and that the relation between the size of the square and the retinal extent of the aftereffect was linear. The equation of the regression line fitted to Fig. 3 is

$$\text{radius of aftereffect} = 6.17 (\text{size of square}) - 0.51, \quad (1)$$

where the size of the checkerboard square and the radius of the retinal region covered by the aftereffect, measured from the fovea, are both expressed in degrees of visual angle. Equation (1) shows that, for instance, squares subtending 1 deg give an aftereffect extending out to an eccentricity of 5.7 deg ( $6.17 - 0.51$ ) from the fovea.

The retinal extent of the aftereffect allows us to calculate the perceptive fields of the visual channels that mediate the aftereffects. We can now rewrite Eq. (1), exchanging terms on the left- and right-hand sides and incorporating a factor of  $\sqrt{2}$ , to give the diameter of the summation area of the perceptive fields (in minutes of arc) for the aftereffects as a function of retinal eccentricity  $E$  (in degrees):

$$\text{PF diameter} = 13.62E + 6.9. \quad (2)$$

[To avoid inconveniently small numbers in Eqs. (2)–(9), the perceptive fields on the left are expressed in minutes arc, and the eccentricities on the right are expressed in degrees. To convert both sides to the same units, divide the right-hand side by 60.]

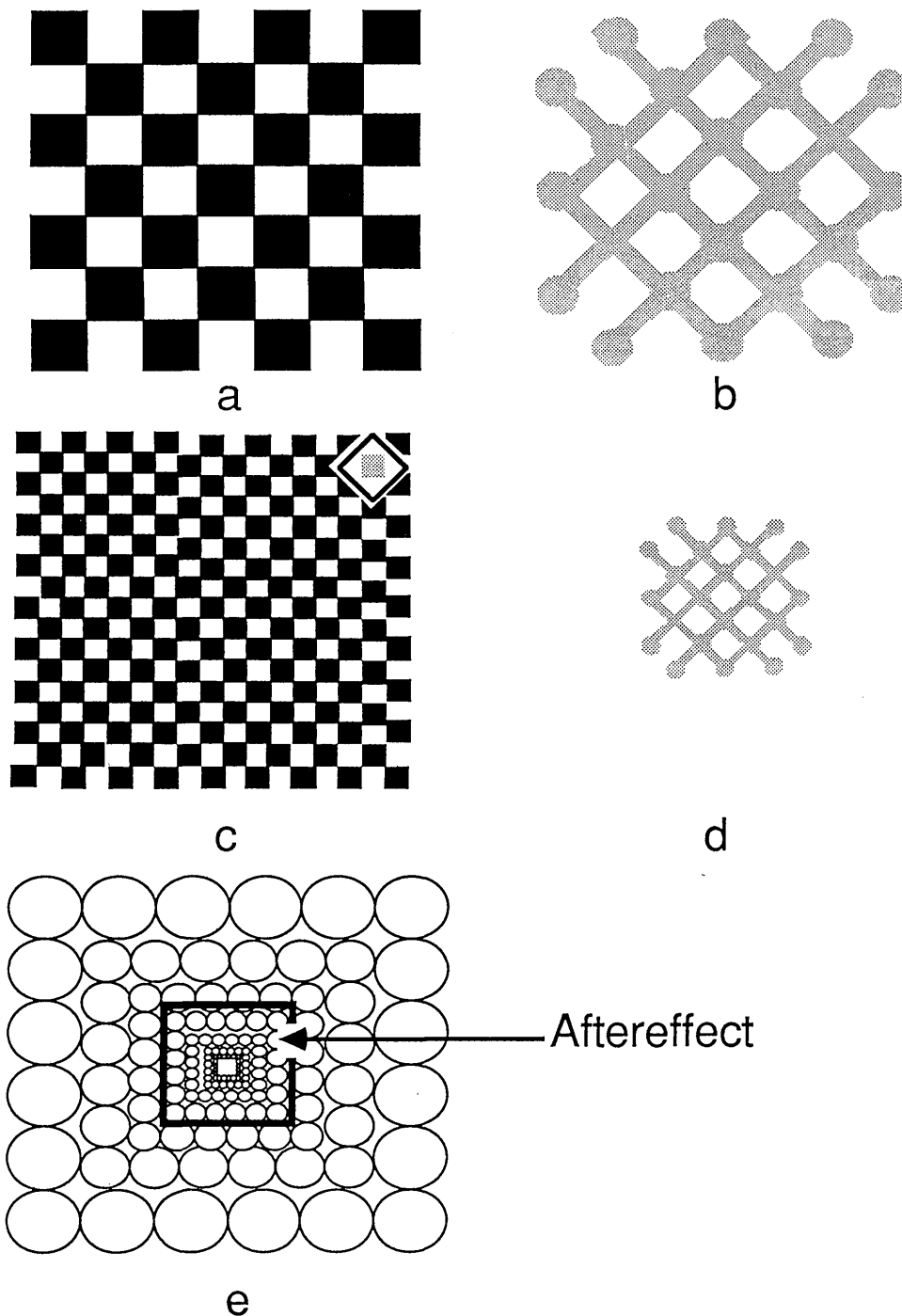


Fig. 2. a, After adaptation by the observer to a checkerboard (left) whose white squares gradually turn black while the black squares gradually turn white, an aftereffect of apparently dimming and brightening regions is seen (right), which looks like an extremely blurred checkerboard. With large checks, a, the aftereffect, b, fills the whole stimulated region, but with small checks, c and d, it fills only a limited region near the fovea. The diamond superimposed upon the checkerboard in c shows a hypothetical perceptive field that sees equal areas of black and white and hence yields no net aftereffect. e, The hypothesis is that aftereffects are seen only in the central retinal region where the perceptive fields (circles) are smaller than the adapting checkerboards.

The data from Fig. 3 are replotted in Fig. 4.<sup>10-14,16-18</sup> The perceptive fields of the transient channels are really very large. For comparison we include psychophysical data from several sources on minimum-separable acuity,<sup>10-13</sup> perceptive fields in the Hermann grid,<sup>14,15</sup> and physiological measures of the diameters and separations of the receptive field of monkey retinal ganglion cells.<sup>16,17,19</sup> All retinal eccentric-

ities ( $x$ ) are plotted in degrees of visual angle, and acuity measures ( $y$ ) are plotted in minutes of arc.

The minimum angle of resolution (MAR) has been measured with Landolt C's<sup>11</sup> and with gratings.<sup>10,13</sup> As a measure of acuity we have replotted<sup>13</sup> the reciprocal of the highest spatial frequency ( $SF_{max}$ ) resolved at each eccentricity ( $MAR = 30/SF_{max}$ ).

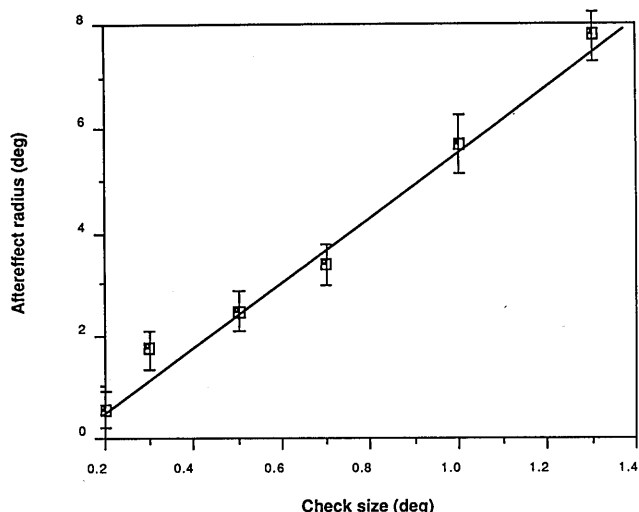


Fig. 3. Results of experiment 1: radius of aftereffect from the fovea, in degrees of visual angle, as a function of the size of the checks in the adapting checkerboard. The larger the squares are, the larger the region of the aftereffect is, since the more peripheral regions have larger perceptible fields.

These acuity data can be fitted by the following equations:

$$\text{MAR} = 0.69E + 1.04 \text{ (Ref. 10),} \tag{3}$$

$$\text{MAR} = 0.84E - 2.65 \text{ (Ref. 11),} \tag{4}$$

$$\text{MAR} = 0.43E + 0.09 \text{ (Ref. 13).} \tag{5}$$

Snellen acuity data at different eccentricities<sup>12</sup> have a slope about five times steeper than the MAR data because letter heights, which are plotted in Fig. 4, are five times the stroke width for Snellen letters:

$$\text{MAR} = 2.76E - 1.86 \text{ (Ref. 12).} \tag{6}$$

Figure 4 also includes measurements on the diameter (square root of the area) and separation of RF's in monkey retinal ganglion cells. Our perceptible fields have diameters four or five times larger than the RF's<sup>16</sup> that can be fitted by

$$\text{RF diameter} = 3.0E + 16.53 \text{ (Ref. 16),} \tag{7}$$

which in turn are about 16 times larger than the separation between monkey ganglion cell RF's:

$$\text{RF diameter} = 0.18E + 0.74 \text{ (Ref. 17).} \tag{8}$$

The fact that the diameter of each of the individual RF's is 16 times their mean separation suggests densely overlapping RF's in which a typical retinal receptor contributes to 256 (16<sup>2</sup>) ganglion cell RF's. RF overlap has been reviewed.<sup>20</sup>

We can estimate the MAR as the mean of the slopes in Eqs. (3)–(5). This mean is equal to 0.653. This result suggests that the perceptible fields underlying our dimming or brightening aftereffects are 20.86 times (13.62/0.653) wider than those underlying acuity, so their areas are about 430 times as large. Presumably these transient visual pathways are few in number and provide only a coarse spatial sampling of the visual image, equivalent to an acuity of worse than 20/400. Figure 5 indicates graphically how coarse these chan-

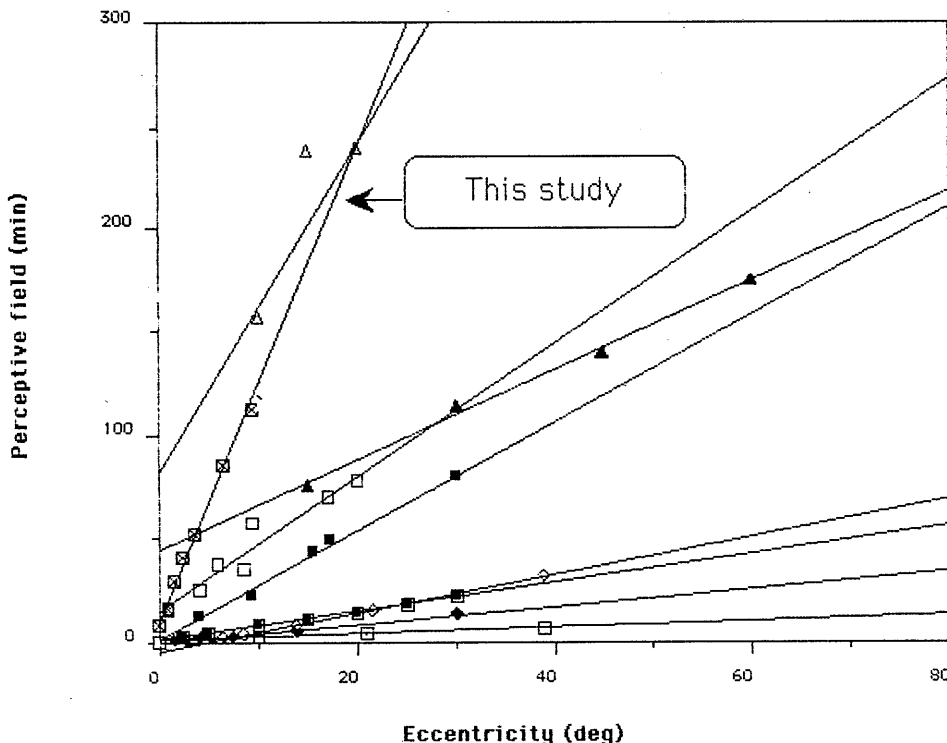


Fig. 4. Data of Fig. 3, replotted (□) to show the diameter of summation areas in the aftereffects, expressed in minutes of arc. Acuity data (MAR's) shown are those of Wertheim<sup>10</sup> (■), Weymouth<sup>11</sup> (◇), Anstis<sup>12</sup> (▲), and Rovamo *et al.*<sup>13</sup> (◆); at all eccentricities the diameters of our perceptible fields are 20 times larger than the mean MAR. The diameter of RF's of monkey retinal ganglion cells<sup>16</sup> and their separations<sup>17</sup> (□) are also shown. Spillmann's<sup>14</sup> perceptible fields (▲), calculated from the optimum size of Hering grids, were comparable in size to the ganglion RF's of Hubel and Wiesel.<sup>16</sup> Finally, the only perceptible field as large as ours comes from the perceived extent of apparent motion in the fine-grain motion illusion<sup>18</sup> (△).

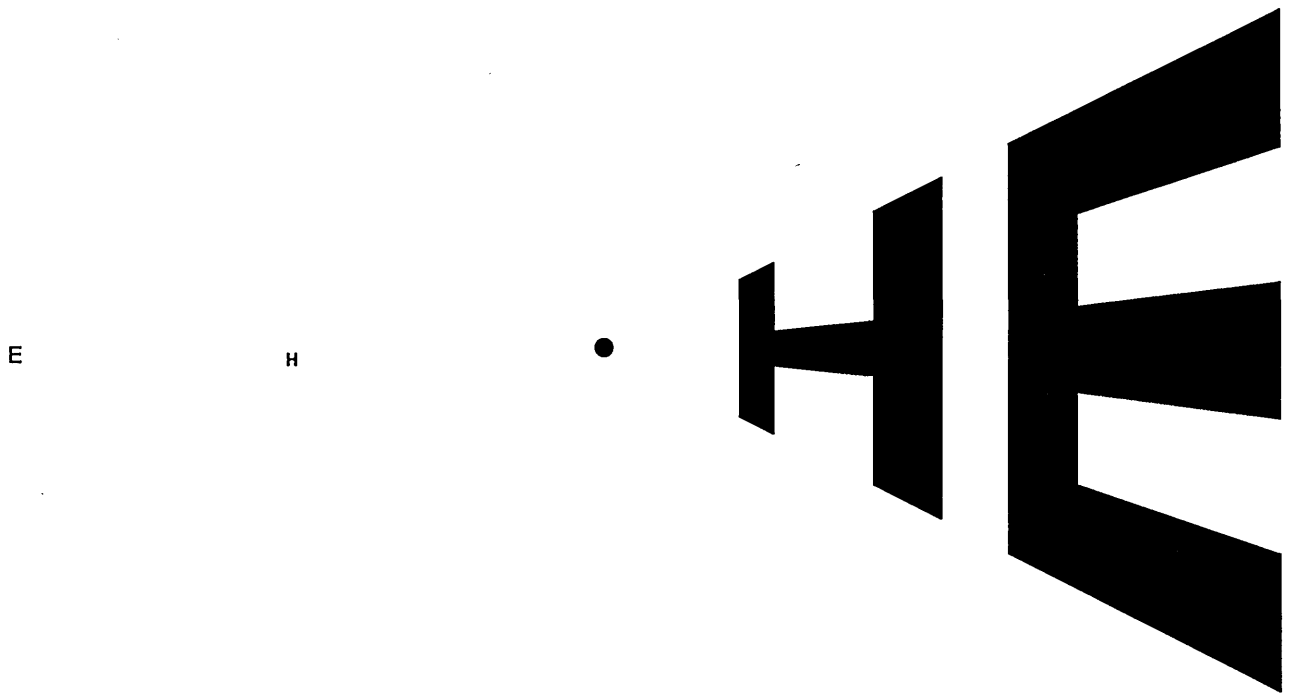


Fig. 5. When the central dot is fixated, the letters on the left should be just at the limit of resolution (as described in Ref. 12). Letters on the right should be just resolvable by the low-acuity visual channels that respond to changing luminance. The large size of these letters indicates large perceptive field sizes, and their perspectivelike distortion indicates a rapid increase in field size with retinal eccentricity.

nels probably are; a person equipped with nothing but these visual pathways might be extremely good at detecting changes in the light level, such as when the Sun goes behind a cloud, but his acuity would be so low that he would be legally blind!

Evidently, our results are not an experimental artifact from eye movements, since eye movements might shift the curve of our results bodily upward but they could not steepen its slope.

The only report of perceptive fields that are as large as ours comes from an illusory expansion of apparent motion seen in the peripheral retina, known as the fine-grain motion illusion.<sup>18,21</sup> When two luminous points, spaced only a few minutes of arc apart, were presented briefly in rapid sequence, subjects reported that a single dot appeared to move over a path of considerable extent. This path length varied from about 2 to 6 deg as the eccentricity was increased from 10 to 24 deg. However, when mapped onto the visual cortex by means of the human cortical magnification factor, the illusion spanned a patch of cortex about 3 mm in diameter, regardless of stimulus eccentricity; such a region in primate visual cortex corresponds approximately to the array of cortical cells that see a given retinal point.

The perceived length of the motion path at different eccentricities is plotted in Fig. 4. The best-fitting line is

$$\text{Apparent path length} = 13.68E + 16.24 \text{ (Ref. 18).} \quad (9)$$

This slope is very close to ours.

Although the fine-grain motion illusion is not fully understood, it is undoubtedly related to the size of RF's. Note that when the two closely spaced dots were presented simultaneously instead of successively to the peripheral retina, they could not be resolved, and only one stationary dot was seen. Position in the peripheral retina may be coded by

relative activity levels in large, overlapping RF's, much as wavelength is coded by the relative responses of broadly tuned R, G, and B cones. Two simultaneous dots are perceptually fused into one dot, but successive dots are clearly resolvable, and analogously a patch of mixed red and green light is metamericly fused into yellow, but the successive colors can be clearly seen in a patch that changes from red to green. Positional metamerism has been discussed,<sup>22,23</sup> and the relationships among peripheral acuity, retinal grain, and cortical magnification factor have been examined.<sup>15-17,20,24-28</sup>

In any event, at all eccentricities our perceptive fields were 4 or 5 times larger than the receptive fields of retinal ganglion cells and 20 times larger than the minimum angle of resolution. Thus the visual pathways that sense a gradual change in luminance have a very coarse spatial grain.

Experiment 1 showed that the spatial summation areas for the aftereffects were 7 arcmin in diameter in the fovea. The next two experiments converge, by means of two complementary methods, on an estimate of 9 arcmin for foveal summation areas. These three independent estimates are in good agreement. We exploited the fact that spatial pooling tends to enhance the signals of space-averaged luminances rather than those of local luminances. In experiment 2 each local point gradually brightened (or dimmed), but the space-averaged luminance did not, so that spatial pooling would emphasize the unchanging space-averaged luminance and reduce any aftereffects. Conversely, in experiment 3 the space-averaged luminance gradually increased (or decreased), but at each local point it did not, so that spatial pooling would emphasize the gradually changing space-averaged luminance and would enhance any aftereffects. Incidentally, the aftereffects in experiments 2 and 3 were much weaker than in experiment 1.

### Experiment 2: Phase-Scrambled Display Gives Aftereffect for Large Pixels Only

Experiment 2 was designed to make the local luminance at each point gradually increase (or decrease) while the space-averaged luminance was held virtually constant. The display was a  $10 \text{ deg} \times 10 \text{ deg}$  region of the TV screen divided into four adjacent 5-deg squares whose inner corners touched at a central fixation point. Each square was divided into pixels whose sizes were set on different trials to 4.5, 9, 18, 36 or 72 arcmin. (Obviously, the smaller the pixel size, the more pixels there are per square.) Note that pixels refers to the stimulus elements whose size was varied in different trials, not to the resolution limits of the computer display.

All the pixels within the northwest and southeast squares gradually increased in luminance, and all the pixels within the other two squares gradually decreased in luminance. The temporal phase of each ramping pixel was randomized by programming the computer to start and stop each pixel at a different height up its temporal luminance ramp (Fig. 6).

The pixels within the two brightening squares gradually stepped up through 16 grey levels and then fell instantly to a minimum and recycled, but each pixel was out of step with its neighbors. Pixels within the dimming squares followed the opposite sequence and were also out of step with their neighbors. This had two consequences:

(1) A snapshot taken of this display at any instant of time would show a random-dot field of small pixels of 16 different grey levels spatially jumbled together, with no 5-deg squares visible. The phase randomization deleted all information about the presence of the 5-deg squares from any single time frame; the squares were perfectly camouflaged, since they existed not at any given instant of time but only as a phase relationship between successive time frames and logically could emerge only during a serial presentation of two or more frames over time.

(2) Within the region of brightening pixels the mean luminance of the screen averaged across many pixels remained virtually constant, because at each tick of the clock

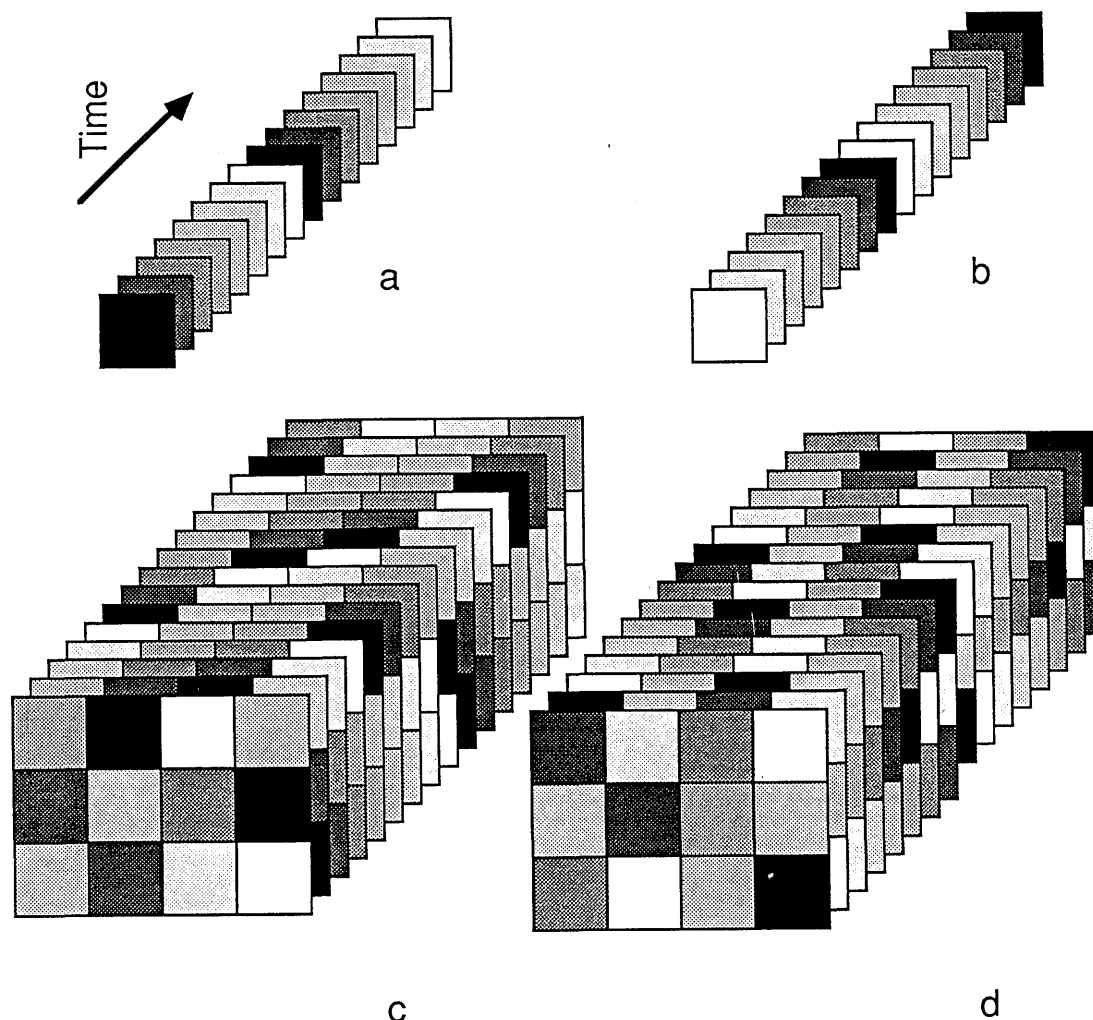


Fig. 6. Phase-scrambled display used in experiment 2. a, A brightening pixel. b, A dimming pixel. Time recedes into the page away from the reader. c, A  $4 \times 3$  array of the brightening pixels shown in a. d, A  $4 \times 3$  array of the dimming pixels shown in b. The front faces of c and d show the spatial array of pixels of random luminances visible at an instant of time. Inspection of the side faces shows that each pixel in c gradually brightens and each pixel in d dims, repetitively over time. Thus each pixel within a stimulus is modulated in the same direction, but the temporal phase of each pixel has been randomized. As a result, when the pixels are smaller than a summation area, no aftereffects are seen.

every pixel increased by one luminance level up the 16-level ramp, except that 1 pixel in every 16 fell abruptly from maximum to minimum luminance. Although each pixel ramped repetitively upward, the space-averaged luminance did not.

After 30 sec of adaptation to the random-phase ramping display, the TV screen was switched to a uniform gray test field, and subjects were asked to report whether they saw any aftereffect. When aftereffects were seen, they were weaker than in experiment 1 and lasted 1–3 sec.

We predicted aftereffects from large pixels but not from small pixels, whose space-averaged luminance (after spatial summation) would remain virtually constant. The summation area can be calculated from the pixel size that was just large enough to give an aftereffect.

As predicted, aftereffects were reported for large pixels but not for small pixels. The mean pixel diameter at which an aftereffect was just reported (mean of five subjects, two trials each) was 9 arcmin. This suggests that the diameter of the summation areas must be 9 arcmin or smaller. If the summation area contained just one pixel, the ramping luminance would generate an aftereffect. If the summation area were large enough to contain  $n$  pixels, with each ramping in random phase, it would average them into a series of  $n$  small, brief ramps, in practice, short staircases of the same slope as the single ramp but containing fewer luminance steps, which would degrade the aftereffect. Thus enlarging the summation areas (increasing  $n$ ) would push the aftereffects below threshold. Therefore the upper bound for the estimated summation area is 9 min ( $n = 1$ ).

Incidentally, we observed that the 5-deg adapting squares were virtually invisible, not only in a static frame but also during the first 10 or 20 sec of inspection of the dynamic visual stimulus. It was almost impossible to make out the squares of brightening pixels and to segregate them perceptually from the squares of dimming pixels. The stimulus looked simply like a field of randomly twinkling pixels. For some reason long inspection times (>20 sec) enhanced the subjective contrast of dimming pixels and diminished that of brightening pixels, which took on a washed-out brownish-sepia appearance. This subjective color allowed the observer to infer the presence of the camouflaged squares. Although the adapting 5-deg squares were themselves invisible or camouflaged, they still gave rise to a visible aftereffect, provided that the pixels exceeded 8 arcmin.

### Experiment 3: Snowfall Display Gives Aftereffect for Small Pixels Only

In the phase-scrambled display just described, each individual pixel gradually brightened or dimmed over time, but the space-averaged luminance remained constant. Conversely, in experiment 3 each individual pixel was either on or off at any given time, but the space-averaged luminance did gradually increase or decrease over time. Thus the temporal luminance ramp did not exist locally within any pixel but was distributed spatially across many pixels.

Imagine a black slate lying on the ground during a steady fall of snow (Fig. 7). White snowflakes land randomly on the black slate and lie there without melting, so the black slate gradually becomes white all over. The slate is then abruptly wiped clean and the cycle begins again. The space-

averaged luminance of the slate gradually increases from black to white along a temporal ramp, but any individual pixel on the slate is initially black, then changes abruptly to white when a snowflake lands on it and remains white for the rest of the cycle, so that its luminance varies according to a rectangular waveform that is symmetrical with respect to time, showing no net gradual dimming or brightening over time. A pixel that received a snowflake early (Fig. 7b) or late (Fig. 7c) in the cycle would have a high (or low) on/off ratio, being white for more (or less) of the cycle. But no individual pixel would know about the temporal ramp, because this ramp information simply does not exist at any one spatial point but consists of a temporal relationship averaged spatially across many pixels. (For a dimming ramp the luminance relationships were reversed; imagine a sheet of white paper under a steady fall of soot.)

The snowfall/sootfall display was presented as a quartet of adjacent 5-deg squares abutting a central fixation point, as before, with the northwest and southeast squares gradually brightening under a snowfall and the other two squares gradually dimming under a sootfall. One pixel now represented one snowflake or soot particle. The luminance ramp was 14 steps high, with 7.14% of the pixels changing from black to white at each step. The ramp repetition rate was 1.63 Hz, and the pixel sizes were 2.25, 4.5, 9, 18, 36, or 72 arcmin in different trials.

In this display the 5-deg squares, defined by the accumulating snow or soot, emerged clearly as salient regions of gradually increasing or decreasing overall luminance. There was no camouflaging of the 5-deg squares as with the phase-scrambled display. As before, the lightening and darkening 5-deg squares did not exist within one time frame but logically could emerge from only two or more successive frames presented serially. Thus sensing of the gradual luminance changes and adaptation to them required comparisons across both space and time: spatial integration across many pixels to extract the space-averaged luminance, and temporal differentiation to sense the rising and falling ramps of luminance. The fact that we did obtain aftereffects from this display shows that both processes were occurring in the visual system.

As before, after 30 sec of observer adaptation to the snowfall/sootfall display the TV screen was switched to a uniform gray test field, and subjects were asked to report whether they saw any aftereffect. When aftereffects were seen, they were weaker than in experiments 1 and 2 and lasted 1–3 sec. Subjects reported that the aftereffects looked stronger in the periphery than in the fovea.

We predicted no aftereffect from large pixels, which were simply turning on and off, but visible aftereffects from small pixels, whose space-averaged luminance (after spatial summation) gradually increased or decreased. The summation area can be calculated from the pixel size that was just small enough to give an aftereffect.

As predicted, aftereffects were reported for small pixels but not for large pixels. The mean pixel diameter at which an aftereffect was just reported (mean of five subjects, two trials each) was 9 arcmin. This suggests that the diameter of the summation areas must be 9 arcmin or larger. If the summation area contained just one pixel, it would detect not a ramp but a pixel turning on and off, which would give no aftereffect. If the summation area were large enough to

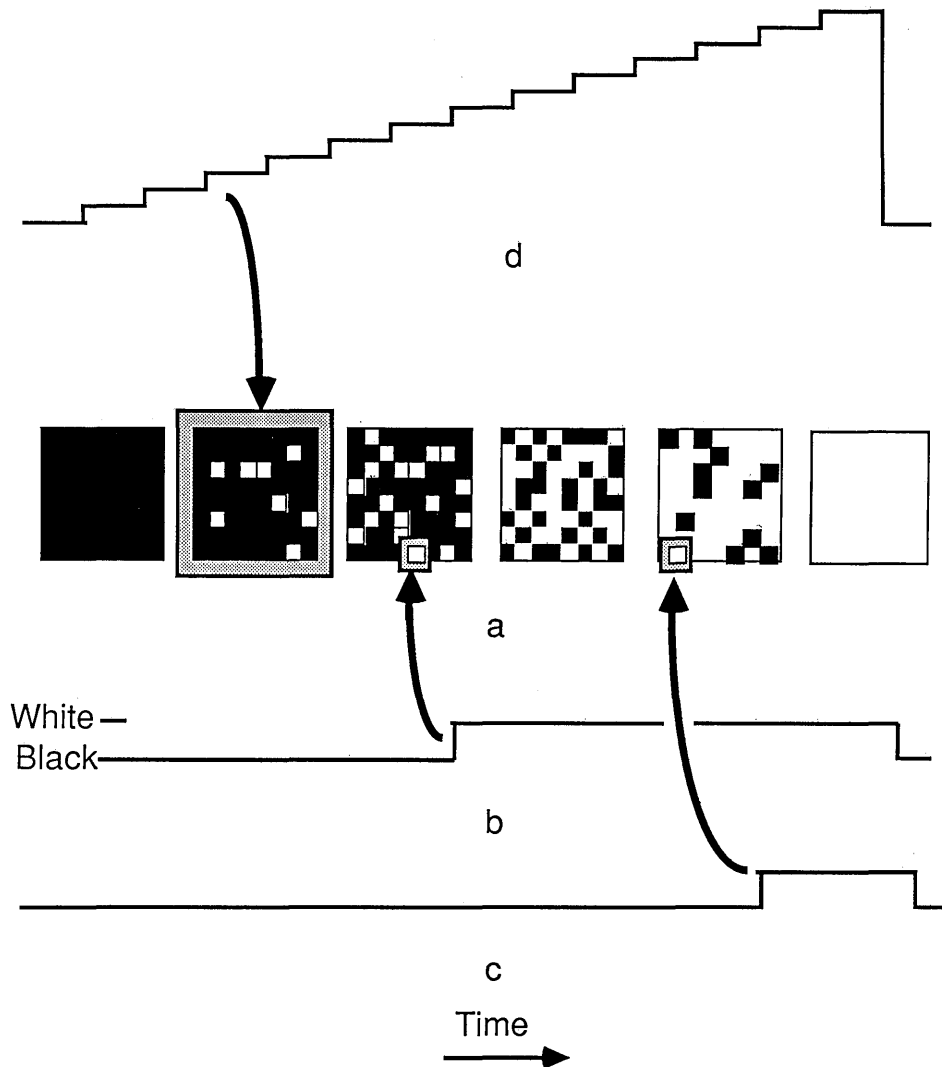


Fig. 7. Snowfall display used in experiment 3. a, An adapting black square gradually fills with randomly placed white pixels. b and c, Any local point is initially black and then switches to white at a random time and resets at the end of the cycle. Local luminances do not change gradually in a way that would lead to an aftereffect. However, the space-averaged luminance, d, does. As a result, when the pixels are small enough to be integrated by a summation area, an aftereffect is seen.

contain  $n$  pixels, it would receive a staircase of up to  $n$  luminance steps, giving a better stimulus staircase as  $n$  increased. Therefore enlarging the summation areas (increasing  $n$ ) would push the aftereffects well above threshold. Thus the lower bound for the estimated summation area is 9 min ( $n = 1$ ). This explains why the aftereffect was more pronounced in the periphery, where the summation areas are larger and  $n$  is therefore greater.

To summarize, aftereffects were produced by the phase-randomized display of experiment 2 only if the pixels were large and by the snowfall display of experiment 3 only if the pixels were small. This was as expected, since in the phase-randomized display the local pixels ramped but the space-averaged luminance did not, so spatial integration across small pixels obliterated the gradual luminance change and the aftereffect. In the snowfall display the space-averaged luminance ramped but the local pixels did not, so spatial integration across small pixels signaled a rising or falling mean luminance and facilitated the aftereffect.

Thus experiments 2 and 3 converge in their estimates of

the foveal summation area. Experiment 2 established an upper bound and experiment 3 established a lower bound of 9 arcmin each. These two converging estimates, derived from foveal threshold aftereffects, agree well with the estimate of 7 arcmin obtained in experiment 1 by extrapolation from extrafoveal suprathreshold aftereffects.

#### Experiment 4: The Brightening Aftereffect from Dimming Fields Is Stronger Than the Dimming Aftereffect from Brightening Fields

We demonstrated an asymmetry between the brightening and dimming aftereffects by splitting the adapting checkerboard into two halves. In both halves of the field only half of the squares varied in luminance, and these luminance-modulated squares were interleaved with mid-gray squares that remained at a fixed reference luminance of  $28 \text{ cd m}^{-2}$ . The squares that changed in luminance were dimming in the left half but brightening in the right half. Both halves produced a plaid or gingham pattern of aftereffects on a gray test field, as before, but the aftereffect pattern was noticeably stronger

on the left half, where dimming squares produced a brightening aftereffect, than on the right, where the opposite was true.

We cannot explain this asymmetry between the aftereffects, although it may be connected with the washed-out sepia appearance of brightening pixels that was mentioned earlier. We have previously noted a similar asymmetry in audition: after adaptation of the subject to a tone whose amplitude was modulated by a falling ramp so that it grew repetitively softer, a steady test tone appeared to be getting louder, and vice versa.<sup>29</sup> Moreover, the apparent loudening that followed adaptation to a softening tone was greater than the apparent softening that followed adaptation to a loudening tone.

#### Experiment 5: No Interocular Transfer

Subjects adapted monocularly for 5 min to a checkerboard of 5-deg squares, as used in experiment 1. The adapted eye then showed a strong aftereffect, as one would expect. However, when a gray test field was viewed with the unadapted eye, no trace of aftereffect could be seen. Thus the aftereffects of brightening and dimming showed no interocular transfer.

#### Experiment 6: Opposite Aftereffects in the Two Eyes

Opposite aftereffects could be built up in the two eyes by simultaneous adaptation in opposite directions.<sup>30,31</sup> The left eye viewed a bipartite field, with a vertical border running through the fixation point, in which the left half was brightening and the right half was dimming. At the same time the right eye viewed a bipartite field in which the left half was brightening and the right half was dimming. The fixation points seen by each eye were fused binocularly, and the rest of the field showed binocular rivalry. After 60 sec of adaptation the subject viewed a gray test field with each eye in alternation and obtained weak aftereffects that were of opposite sense in the two eyes. In the left eye the aftereffect was of dimming on the left and brightening on the right. The opposite aftereffect was seen by the right eye. No aftereffects were seen when both eyes viewed the test field.

Taken together, experiments 5 and 6 show that the aftereffect arose in visual channels that received monocular inputs.

## DISCUSSION

Presumably, the aftereffects result from adaptation of transient on and off channels. The transient response to a temporal luminance ramp is illustrated in Fig. 8 as  $dl/dt$ , the difference between the current stimulus and a slightly time-delayed copy<sup>6</sup>; there is a weak on response (shown as positive) to the gradually rising luminance, followed by a stronger off response (shown as negative) to the briefer, but steeper, falling portion of the ramp. (It makes no difference to the argument here whether on and off are signaled in separate channels<sup>32</sup> or by positive and negative responses within a single channel.) If the transient channels were linear, the on and off responses would exactly cancel out over one cycle of the stimulus, leading to no net adaptation and no aftereffects. If the transient responses are nonlinear, however, the on and off responses may not exactly cancel out, and adaptation can occur. Studies of illusory brightness shifts in drift-

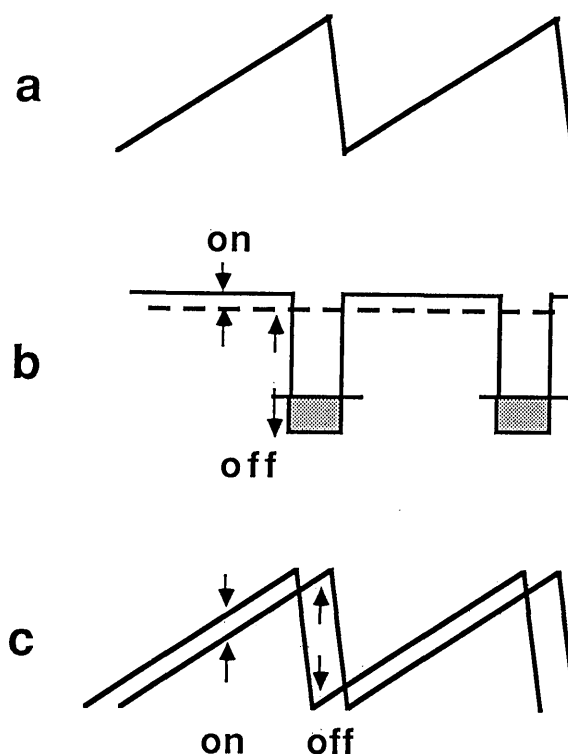


Fig. 8. a, Temporal luminance ramp. b, The transient response reflects the steepness of the slope, with positive slope signaled by transient on channels and negative slope by transient off channels. The total on response will balance the total off response if the responses are linear. If there is a saturation of the transient response, the smaller on responses are less likely to reach the saturation region than the larger off responses (the shaded, or clipped, portion of the negative off response in b has exceeded the saturation limit). c, The manner in which the transient response, a response to change, can be visualized as a difference between the current luminance value and the previous ones.<sup>6</sup>

ing ramp gratings<sup>6</sup> indicate a saturation of the larger off response to the sharp fall in the luminance ramp (Fig. 8b). Therefore the net on response is significantly larger than the net off response and undergoes adaptation during exposure to a gradually rising ramp. A gradually falling ramp leads to the opposite adaptation.

The visual channels described here respond to temporal luminance changes and have a coarse spatial grain. These resemble the transient channels<sup>33</sup> that respond to high temporal frequencies and low spatial frequencies, as opposed to sustained channels that have the opposite properties. Presumably, the channels sensitive to increasing luminance receive inputs from on-center ganglion cells, and channels sensitive to decreasing luminance receive inputs from off-center ganglion cells. The aftereffects were monocular, showing no interocular transfer, so they could be retinal. Alternatively, if they are postretinal, they might arise in monocularly driven neurons that lie in either the visual cortex or the midbrain.

In the macaque the retinal output to the dorsal lateral geniculate nucleus (LGN) is conveyed primarily by two major classes of ganglion cell. One class (P-like ganglia) consists of neurons with small RF's, slow conduction velocity, and color-opponent responses. The other class (M-like ganglia) consists of neurons with larger RF's, faster conduction velocity, and broadband responses.<sup>28</sup> In the dorsal LGN

these two cell classes segregate into the parvocellular (P) and magnocellular (M) layers. There seems to be a 1:1 ratio between the retinal and geniculate neurons, and P cells are about 10 times more numerous than M cells. The sensitivity of M cells to luminance but not to hue, their large RF's, and their small numbers (which could indicate undersampling of the visual field) make them prime candidates as a substrate for our aftereffects.

It is hard to find any cortical structures with domains large enough to match the coarse spatial grain of our aftereffects, but one possible candidate might be the cortical modules associated with cytochrome oxidase puffs. The histochemical visualization of a regular pattern of vertical puffs of high cytochrome oxidase activity has provided an anatomical basis for the suggestion that the macaque striate cortex (area V1) is composed of an array of functional units or modules.<sup>34</sup> The visual-field area of a puff-centered module has been calculated to be 0.01 deg<sup>2</sup> at an eccentricity of 1 deg and 3.0 deg<sup>2</sup> at an eccentricity of 40 deg.<sup>28</sup> Our aftereffects have a coarser spatial grain than this and would have an extrapolated area of 7.3 deg<sup>2</sup> at an eccentricity of 40 deg.

Another possible site for the aftereffects is the midbrain. The pretectal area of the midbrain receives the visual input for the pupillary control system. Visual neurons controlling the pupil would need to respond to the space-averaged luminance of the retinal image, and such units have been found in the pretectal area of the cat.<sup>35</sup> Some cells, luminance detectors, increased their firing rate, and others, darkness detectors, decreased their firing rate as the steady level of luminance was increased. More important, other cells responded transiently to the onset or offset of illumination, possibly to ensure a brisk pupil response. Adaptation of these transient cells could conceivably underlie our aftereffects. These units are monocularly driven, which is surprising if they control the binocular consensual pupil response but is consistent with the fact that our aftereffects are monocular, showing no interocular transfer. W ganglion cells have been described as possible luminance detectors,<sup>36</sup> and these project to the midbrain, not to the LGN.<sup>37</sup> Certainly, the very coarse spatial tuning of our aftereffects is not inconsistent with a midbrain site.

Visual units with poor spatial acuity but good sensitivity to a gradual luminance change would have evolutionary value. They could detect sudden changes in light level, which can signal the onset of danger, such as a predator looming. Also, the retinal image constantly fluctuates in luminance whenever objects of invariant reflectance undergo random changes in illumination, say, when clouds move across the Sun. Direct sensing of these random changes permits them to be separated out so that irrelevant details about temporary illumination can be discarded and the important information about invariant properties of objects, such as their reflectances, is left intact.

## ACKNOWLEDGMENTS

This work was supported by grant A0260 from the Natural Sciences and Engineering Research Council of Canada. We thank Loretta Bateman and Simone Swimmer for their assistance in collecting the data; Stan Schein for helpful discussions; and Marc Green, Ian Howard, and Patrick Cavanagh for commenting on the manuscript.

## REFERENCES

1. S. M. Anstis, "Visual adaptation to gradual change of intensity," *Science* **155**, 710-712 (1967).
2. J. Krauskopf, "Discrimination and detection of changes in luminance," *Vision Res.* **20**, 671-677 (1980).
3. M. Hanly and D. M. Mackay, "Polarity-sensitive perceptual adaptation to temporal sawtooth modulation of luminance," *Exp. Brain Res.* **35**, 37-46 (1979).
4. S. M. Anstis, "Aftereffects of form, motion, and color," in *Sensory Experience, Adaptation, and Perception: Festschrift for Ivo Kohler*, L. Spillmann and B. R. Wooten, eds. (Erlbaum, Hillsdale, N.J., 1984), pp. 583-601.
5. S. M. Anstis, "Interactions between simultaneous contrast and adaptation to gradual luminance change," *Perception* **8**, 487-495 (1978).
6. P. Cavanagh and S. M. Anstis, "Brightness shift in drifting ramp gratings isolates a transient mechanism," *Vision Res.* **26**, 899-908 (1986).
7. S. M. Anstis, "Recovering motion information from luminance," *Vision Res.* **26**, 147-160 (1986).
8. S. M. Anstis, "Visual stimuli on the Commodore Amiga: a tutorial," *Behav. Res. Methods Instrum. Comput.* **18**, 535-541 (1986).
9. G. S. Brindley, "Two new properties of foveal afterimages and a photochemical hypothesis to explain them," *J. Physiol. (London)* **164**, 168-179 (1962).
10. T. Wertheim, "Über die indirekte Sehscharfe," *Z. Psychol. Physiol. Sinnesorg.* **7**, 172-189 (1894).
11. F. W. Weymouth, "Visual sensory units and the minimal angle of resolution," *Am. J. Ophthalmol.* **46**, 102-113 (1958).
12. S. M. Anstis, "A chart demonstrating variations in acuity with retinal position," *Vision Res.* **24**, 589-592 (1974).
13. J. Rovamo, V. Virsu, and R. Nasanen, "Cortical magnification factor predicts the photopic contrast sensitivity of peripheral vision," *Nature* **271**, 54-55 (1978).
14. L. Spillmann, "Zur Feldorganisation der visuellen Wahrnehmung beim Menschen," Ph.D. dissertation (Westfälische Wilhelms Universität Münster, Münster, Federal Republic of Germany, 1964).
15. A. Ransom-Hogg and L. Spillmann, "Perceptive field size in fovea and periphery of the light and dark-adapted retina," *Vision Res.* **20**, 221-228 (1980).
16. D. H. Hubel and T. N. Wiesel, "Uniformity of monkey striate cortex. A parallel relationship between field size, scatter, and magnification factor," *J. Comp. Neurol.* **158**, 295-306 (1974).
17. P. M. Daniel and D. Whitteridge, "The representation of the visual field on the cerebral cortex in monkeys," *J. Physiol. (London)* **159**, 203-221 (1961).
18. D. H. Foster, J. Thorson, J. T. MacIlwain, and M. Biederman-Thorson, "The fine-grain movement illusion: a perceptual probe of neuronal connectivity in the human visual system," *Vision Res.* **21**, 1123-1128 (1981).
19. E. T. Rolls and A. Cowey, "Topography of the retina and striate cortex and its relationship to visual acuity in rhesus monkeys and squirrel monkeys," *Exp. Brain Res.* **10**, 298-310 (1970).
20. B. M. Dow, A. Z. Snyder, R. G. Vautin, and R. Bauer, "Magnification factor and receptive field size in foveal striate cortex of the monkey," *Exp. Brain Res.* **44**, 213-228 (1981).
21. M. Biederman-Thorson, J. Thorson, and G. D. Lange, "Apparent movement due to closely spaced sequentially flashed dots in the human peripheral field of vision," *Vision Res.* **11**, 889-903 (1971).
22. I. P. Howard, *Human Visual Orientation* (Wiley, New York, 1982).
23. S. M. Anstis, "Visual coding of position and motion," in *Biological Processing of Images*, O. J. Braddick and A. C. Sleigh, eds. (Springer, New York, 1983), pp. 177-195.
24. A. Cowey and E. T. Rolls, "Human cortical magnification factor and its relation to visual acuity," *Exp. Brain Res.* **21**, 447-454 (1974).
25. J. Rovamo and V. Virsu, "An estimation and application of the human cortical magnification factor," *Exp. Brain Res.* **37**, 495-510 (1979).
26. V. Virsu and J. Rovamo, "Visual resolution, contrast sensitivity,

- and the cortical magnification factor," *Exp. Brain Res.* **37**, 475-494 (1979).
27. N. Drasdo, "The neural representation of visual space," *Nature* **266**, 554-556 (1977).
  28. S. J. Schein and F. M. de Monasterio, "The mapping of retinal and geniculate neurons onto striate cortex of macaque," *J. Neurophysiol.* (to be published).
  29. A. H. Reinhardt-Rutland and S. M. Anstis, "Auditory adaptation to gradual rise or fall in intensity of a tone," *Percept. Psychophys.* **31**, 63-67 (1982).
  30. B. P. Moulden, "After-effects and the integration of neural activity within a channel," *Philos. Trans. R. Soc. London* **290**, 39-55 (1980) [reprinted in *The Psychology of Vision*, C. Longuet-Higgins and N. Sutherland, eds. (Royal Society, London, 1980)].
  31. S. M. Anstis and K. Duncan, "Separate motion aftereffects from each eye and from both eyes," *Vision Res.* **23**, 161-169 (1983).
  32. R. Jung, "Visual perception and neurophysiology," in *Central Processing of Visual Information A: Integrative Functions and Comparative Data*, R. Jung, ed. (Springer-Verlag, Berlin, 1973), pp. 1-152.
  33. P. Lennie, "Parallel visual pathways: a review," *Vision Res.* **20**, 561-594 (1980).
  34. H.C. Horton, "Cytochrome oxidase patches: a new cytoarchitectonic feature of monkey visual cortex," *Philos. Trans. R. Soc. London* **304**, 199-253 (1984).
  35. R. J. Clarke and H. Ikeda, "Pupillary response and luminance and darkness detector neurones in the pretectum of the rat," in *Pathophysiology of the Visual System*, L. Maffei, ed. (Junk, The Hague, The Netherlands, 1981).
  36. J. Stone and Y. Fukuda, "Properties of cat retinal ganglion cells: a comparison of W-cells with X- and Y-cells," *J. Neurophysiol.* **37**, 722-748 (1974).
  37. Y. Fukuda and J. Stone, "Retinal distribution and central projections of Y-, X- and W-cells of the cat's retina," *J. Neurophysiol.* **37**, 749-772 (1974).